

Investigation of Temperature-Dependent Tensile Properties of Cu-Ag Nanowires with Varying Ag Content: A Molecular Dynamics Study

Hamimul Islam Chowdhury*, Mohammad Mizanur Rahman

Department of Mechanical Engineering, Chittagong University of Engineering & Technology, Chattogram-4349, Bangladesh

ABSTRACT

Molecular dynamics (MD) simulation has been carried out to explore the influence of temperature and silver (Ag) composition on the tensile properties of single crystalline cylindrical-shaped, face-centered cubic (FCC) Cu-Ag nanowires when subjected to uniaxial tensile strain. The simulations were conducted using LAMMPS (Large-scale Atomic/Molecular Massively Parallel Simulator) simulation package, which is known for its precise characterization of metallic systems and interatomic interactions were defined using MEAM (Modified Embedded Atom Method) potential. The tensile properties, including ultimate tensile strength and modulus of elasticity were determined from the engineering stress-strain curves at temperatures ranging from 200 K to 400 K. The ultimate tensile strength of the nanowires varied between 8.17 GPa and 6.11 GPa, while the modulus of elasticity ranged from 82.52 GPa to 102.42 GPa. The linear elastic behavior was maintained until the strain reached between 0.02 and 0.035. Cu-Ag₂₀ demonstrated a favorable combination of ultimate tensile strength (UTS) and modulus of elasticity, making it a well-balanced choice among the compositions studied. This study sheds light on how varying Ag content and temperature impact the strength and elasticity of Cu-Ag nanowires, which is crucial for designing materials with desired mechanical properties, especially for applications in nano-electromechanical systems (NEMS) and micro-electromechanical systems (MEMS).

Keywords: Molecular Dynamics, LAMMPS, Cu-Ag nanowire, Uniaxial Loading.



Copyright @ All authors

This work is licensed under a [Creative Commons Attribution 4.0 International License](https://creativecommons.org/licenses/by/4.0/).

1. Introduction

Nanowires are minuscule, filamentous entities characterized by their nanometer-scale diameters (10^{-9} m). They fall under the category of one-dimensional (1-D) materials because their length significantly surpasses their width, giving them a high aspect ratio. Nanowires are distinguished by their remarkable flexibility, high tensile strength, and consistent morphology. When it comes to metallic nanowires, they demonstrate a greater magnetic coercivity in comparison to their macroscopic equivalents. In terms of thermoelectric characteristics, metallic nanowires are noted for their elevated Seebeck coefficient, which is attributed to the increased density of electronic states. This results in their superior ability to conduct heat and electricity over bulk materials [1].

A Cu-Ag nanowire is a nanoscale wire made up of both copper (Cu) and silver (Ag), characterized as bimetallic due to its composition of two distinct metallic elements. These nanowires have attracted significant interest due to their unique properties and potential applications [2]. The significant leap in nanowire technology was made by the innovators at Bell Laboratories, who fabricated a nanoscale quantum-well wire, essentially a semiconductor structure composed of exceedingly fine layers [3]. Lee et al. discussed nanowires crucial role in photonics and optoelectronics due to their ability to act as resonators and waveguides in photonic integrated circuits (PICs), which increases the performance of 2D materials used in these circuits for light enhancement and guiding [4]. Stewart et al. described a room-temperature solution-phase process for synthesizing copper-silver (Cu-Ag), copper-gold (Cu-Au), and copper-platinum (Cu-Pt) core-shell nanowires. The process involves using ascorbic

acid to remove the passivating copper oxide coating from Cu nanowires and then reducing noble metal ions onto the Cu nanowires to form the core-shell structure. The Cu-Ag nanowires synthesized via this method possess optoelectronic properties comparable to Ag nanowire films with similar aspect ratio. Moreover, unlike pure Cu nanowires, the Cu-Ag nanowires demonstrate resistance to oxidation in dry air at 160°C and under humid conditions (85% RH) at 85°C for 24 hours. This research is significant because it suggests that Cu-Ag core-shell nanowires could serve as a cost-effective alternative to silver nanowires in the production of transparent conducting films, which are essential components in various electronic devices [5]. In 2014, Ye et al. explored the rapid production of copper nanowires (Cu NW) with high aspect ratios through a process involving ethylenediamine (EDA)-mediated reduction of Cu (II) at atmospheric pressure. This research marked the inaugural disclosure of Cu NW synthesis with an aspect ratio of 5700, the most substantial recorded to date achieved through solution coating. This synthesis, completed in just 30 minutes, is employed in the creation of transparent conductive films boasting a transmittance exceeding 95% and a sheet resistance under $100 \Omega/sq$ [6]. Wei et al. developed oxidation-resistant Cu-Ag core-shell nanowires where Cu nanowires coated with a 20 nm layer of Ag through a simple galvanic replacement reaction, without the need for stirring or heating. The resulting bio-inspired piezoresistive e-skin, which mimics a rose-petal surface on 2D polydimethylsiloxane (PDMS), boasts a low detection threshold (under 2 Pa) and swift response and relaxation times (36ms and 30ms, respectively), along with remarkable sensitivity of 1.35 kPa^{-1} and stability of over 5000 cycles [7]. Yuan et al. fabricated Cu-Ag core-shell nanoparticles using a

*Corresponding Author Email Address: hamimulislam99@gmail.com

one-step wet chemical method. These nanoparticles exhibit a high degree of sphericity with a uniform Ag coating on the Cu nanoparticle surface. Remarkably, these spherical Cu-Ag core-shell nanoparticles maintain thermal stability even at elevated temperatures of 300°C. The electrical sheet resistance of these nanoparticles, when comprising 27.93 wt% Ag, is notably low at 4.03 $\mu\Omega$ cm [8]. Li et al. studied Cu-Ag bimetallic nanowire where uniaxial tensile direction was applied varying shell thickness and temperature. The findings indicate that at temperatures under 500K, a reduction in shell thickness from 1.5 nm to 0.25 nm leads to a transition in the plastic deformation process, shifting from a misfit dislocation tube mechanism to one dominated by surface dislocation nucleation [9]. Sarkar et al. did a Molecular Dynamics approach to investigate the tensile characteristics of Cu-Ag core-shell nanowires. These nanowires had diameters ranging from 9 to 30 nm, with variations in the core diameter, shell thickness, and strain velocity (0.1–6 Å/ps). The research indicated that a strain velocity of 1 Å/ps for a core diameter of 10 nm and a shell thickness of 2 nm resulted in the greatest yield strength and ultimate tensile strength. Conversely, a strain velocity of 6 Å/ps, applied to nanowires with the same core diameter and shell thickness, was associated with the highest Young's modulus [10]. Sarkar et al. also investigated defect and dislocation behaviors during tensile deformation of copper-silver core-shell nanowires varying core diameter and shell thickness. Throughout the deformation process, the Wigner-Seitz defect analysis was utilized to assess the overall count of vacancies and interstitials. Simultaneously, the Dislocation Extraction Algorithm (DXA) was employed to examine the characteristics, quantity, and cumulative length of dislocation segments [11].

Prior investigations have focused on core-shell structures with fixed compositions, leaving a significant gap in the understanding of the tensile behavior of Cu-Ag nanowires with varying Ag content. The present study addresses this deficiency by examining the effects of both Ag content and temperature on these properties. Furthermore, we utilize the MEAM potential, which is more accurate and efficient for metal alloys than the EAM potential used in previous work, enabling more reliable simulations.

2. Methodology

This investigation was conducted using LAMMPS [12] simulation software. In nano-scale, there contains a huge numbers of atomic unit cell, so it become much hard to conduct first principles calculation for numerous numbers of atoms. The cylindrical-shaped nanowire was built from an FCC block using proper lattice parameter by ATOMSK. Substitutional Ag atoms were arbitrarily inserted in the block to get the required concentrations. Then the data file was used for structure definition on LAMMPS. The properties were investigated at temperature 200K to 400K with an interval of 100K. The Ag content was kept between 5 to 40%. Lattice parameters, internal coordinates of atoms were collected to construct the crystal structure of nanowire. Due to the immiscibility of these elements, there were only segregated

configurations of Cu-Ag nanoparticle systems. Post-processing tools such as OVITO [13] and MATLAB [14] were employed to graphically present the collected data.

2.1 Structure

The FCC structure of Cu-Ag nanowire was constructed by using ATOMSK software. Here, the nanowire consists of 23440 atoms. At first, FCC Cu structure of 80×10×10 unit cell was built, then 10% of total atoms were replaced arbitrarily by Ag atom. Lattice parameters of Cu and Ag are listed in Table 1. Sample crystal structure of Cu-Ag₁₀ nanowire shown in Fig.1.

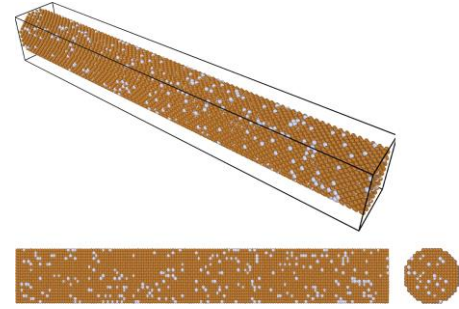


Fig.1 Crystal structure of Cu-Ag₁₀ nanowire

2.2 Potential file

MEAM was used as potential parameters. It is a derived advancement of the embedded atom method (EAM) which adds angular forces. It is well-suited for modeling metals and alloys with fcc, bcc, hcp, and diamond cubic structures. It can also describe materials with covalent interactions, such as silicon and carbon. Formula of total energy for this potential can be written as [15]

$$E = \sum_i \left(F_i(\bar{\rho}_i) + \frac{1}{2} \sum_{i \neq j} \phi_{ij}(R_{ij}) \right) \quad (1)$$

Here, E is the total energy, F_i is the embedding function for an atom i embedded in a background electron density $\bar{\rho}_i$, ϕ_{ij} is the pair interaction energy between atoms i and j separated by a distance R_{ij} .

MEAM potential parameters for Ag and Cu are provided in Table 2 below. The interatomic potential for Cu-Ag was obtained from these parameters. Table 3 [16] presents the parametrization of Cu-Ag system.

Table 1 Lattice parameters and structure size of Cu-Ag FCC.

Lattice Parameter		Dimension of Structure	
a (Å)	3.851	x (Å)	326.32
b (Å)	3.851		
c (Å)	3.851		
$\alpha^{(0)}$	90	y (Å)	40.79
$\beta^{(0)}$	90		
$\gamma^{(0)}$	90		
		z (Å)	40.79

Table 2 MEAM potential parameters for Ag and Cu obtained from potential file.

	E_c	r_e	α	A	$\beta^{(0)}$	$\beta^{(1)}$	$\beta^{(2)}$	$\beta^{(3)}$	$t^{(1)}$	$t^{(2)}$	$t^{(3)}$	C_{\max}	C_{\min}	d
Ag	2.85	2.880	6.01	0.94	4.7	2.2	6.0	2.2	3.4	3.00	1.5	2.80	1.38	0.05
Cu	3.54	2.555	5.15	0.94	3.83	2.2	6.0	2.2	2.72	3.04	1.95	2.80	1.21	0.05

Table 3 Parametrization of Cu-Ag binary system.

Parameter	Selected value
E_c	$0.75E_c^{Cu} + 0.25E_c^{Ag} + C$
r_e	2.71
d	$0.75d^{Cu} + 0.25d^{Ag}$
$C_{min\ or\ max}(Ag - Cu - Ag)$	$1.38 = C_{min\ or\ max}^{Ag}$
$C_{min\ or\ max}(Cu - Ag - Cu)$	$1.21 = C_{min\ or\ max}^{Cu}$
$C_{min\ or\ max}(Ag - Ag - Cu)$	$\left[0.5(C_{min\ or\ max}^{Ag})^{\frac{1}{2}} + 0.5(C_{min\ or\ max}^{Cu})^{\frac{1}{2}}\right]$
$C_{min\ or\ max}(Ag - Cu - Cu)$	$\left[0.5(C_{min\ or\ max}^{Cu})^{\frac{1}{2}} + 0.5(C_{min\ or\ max}^{Ag})^{\frac{1}{2}}\right]$
ρ_0	$\rho_0^{Ag} = \rho_0^{Cu} = 1$

Here, the units of the cohesive energy (E_c), the equilibrium nearest-neighbor distance (r_e) and alpha parameter (α) for pair potential between i^j are eV, Å, and Å respectively. C_{min} or C_{max} are parameters that determine the degree of many-body screening [17].

2.3 LAMMPS Environment

Complete minimization of the crystal structure of Cu-Ag FCC alloy nanowire was done for confirmation of the equilibrium state. Minimization of the energy was done with the help of a conjugate gradient minimization method before performing the simulations. The most time-consuming stage in a MD simulation is the force computation, which involves calculating the force exerted on each atom in the simulation region by all other $n-1$ atoms. In a MD simulation of N atoms, the force calculation increases as n^2 . Cut-off radius ($r_{cut-off}$) was used to reduce computation time, and it is to ignore atoms outside of a sphere of radius. The cut-off radius used in this simulation was 4.5 Å. We used Velocity Verlet algorithm [18] as integration of equations of motions. In this simplified integration method, the velocities, positions, and forces are simultaneously calculated using the following algorithm. At first, r , v and a at time t are used to compute

$$r(t + \Delta t) = r(t) + v(t)\Delta t + \frac{1}{2}a(t)\Delta t^2 \quad (2)$$

Then, $a(t + \Delta t)$ is derived from the interaction potential using new positions $r(t + \Delta t)$. After that, both $a(t)$ and $a(t + \Delta t)$ are used to compute

$$v(t + \Delta t) = v(t) + \frac{1}{2}(a(t) + a(t + \Delta t))\Delta t \quad (3)$$

The time step used in this simulation is 0.001 picoseconds (1 femtosecond). Firstly, constant NVT integration was executed for 50 picoseconds and then the tensile load is applied. After that, NVE ensemble was used for making the system thermally equilibrium and the duration for this process is 50 picoseconds. For controlling the temperature, a Nose-Hoover thermostat [19] was used. Trial and error process was used in purpose of selecting the needed time steps for NVT and NVE simulation for equilibrating state variables. The following equation of virial stress theorem [20] was used for calculating atomic stresses under deformation.

$$\sigma_{ij}^{\alpha} = \frac{1}{\Omega^{\alpha}} \left(\frac{1}{2} m^{\alpha} v_i^{\alpha} v_j^{\alpha} + \sum_{\beta=1}^n r_{\alpha\beta}^i f_{\alpha\beta}^j \right) \quad (4)$$

Where.

α, β = Atomic indices

i, j = Cartesian coordinate system indices

Ω^{α} = Atom α volume

m^{α} = Mass of atoms

v^{α} = Velocity of atom

$r_{\alpha\beta}$ = Atomic distance between α and β

$f_{\alpha\beta}$ = Atomic forces between α and β

The elongation of the NW, e , is defined as:

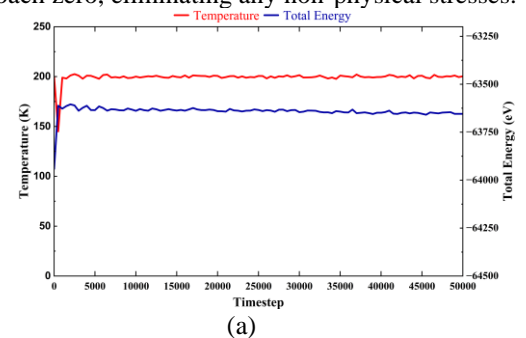
$$e = \frac{l_k - l_0}{l_0} \times 100\% \quad (5)$$

where, l_k is the instantaneous length and, l_0 is the initial length before stress loading.

3. Results and discussion

3.1 Relaxation results

Following the minimization process using NVT and NVE ensembles, the crystal nanowires achieved complete stability. The temperature, total energy, volume, and pressure of the nanostructure at temperatures of 200K, 300K, and 400K were calculated. The energy of the structure was stabilized in the negative zone due to its high negative potential energy and low positive kinetic energy. To stabilize the nanostructures volume and energy, the NVT ensemble was executed. Fig.2 shows that relaxation occurs within the first few thousand timesteps, after which both temperature and total energy fluctuate minimally around their equilibrium values. Equilibration involves energy minimization to achieve a local energy minimum, stabilizing atomic positions. Relaxation allows forces acting on atoms to approach zero, eliminating any non-physical stresses.



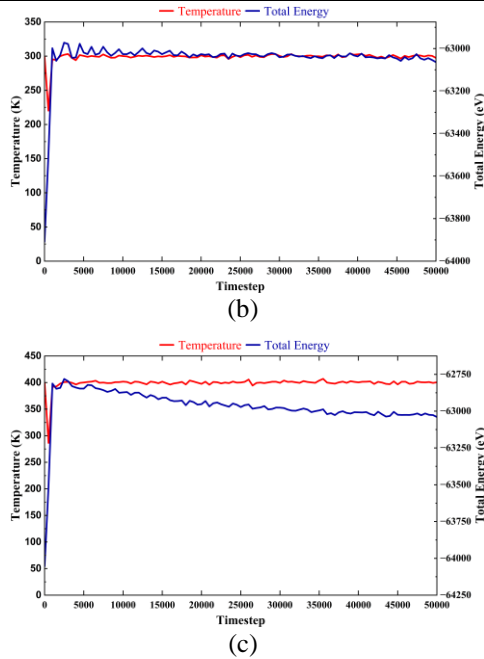


Fig.2 Time steps vs Temperature and Total Energy of Cu-Ag₁₀ at (a) 200K, (b) 300K and (c) 400K.

3.2 Stress-Strain behavior

The stress-strain relationship of the Cu-Ag nanowire was determined by analyzing the curve at a strain rate of 10^{11} s^{-1} . Fig.3 collectively reveals the influence of temperature and silver content on the strength, elasticity, and failure characteristics of the nanowires under uniaxial tensile loading. Across all temperatures, the stress-strain curves exhibit an initial elastic region followed by a sharp increase to a peak stress, representing the ultimate tensile strength (UTS). Beyond this point, the curves gradually decline, indicating plastic deformation and eventual failure.

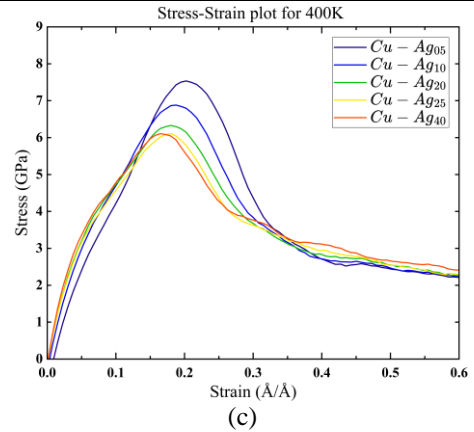
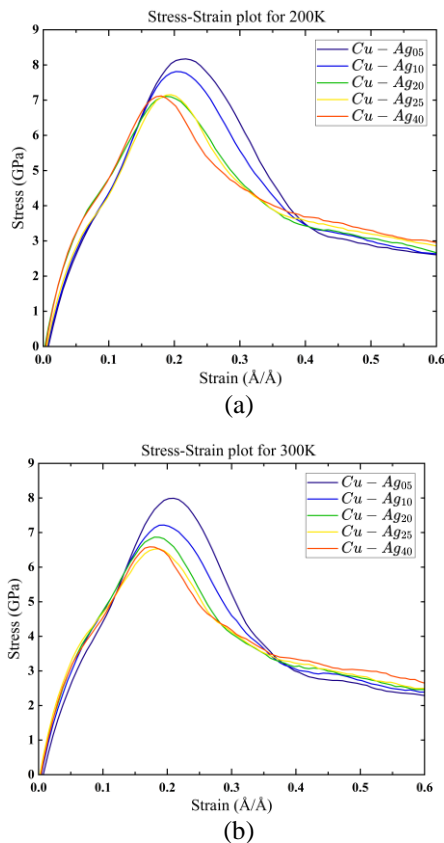


Fig.3 Stress vs. Strain curves of five different Ag content at 200K, 300K and 400K.

3.2.1 Influence of Silver (Ag) Concentration

The peak stress consistently decreases as the Ag content increases across all temperature ranges. Nanowires with lower Ag concentrations (e.g., 5%Ag and 10%Ag) demonstrate higher ultimate tensile strength compared to those with higher Ag levels (e.g., 25%Ag and 40%Ag). This reduction in strength with increased Ag content is due to the disruption of the FCC lattice structure of Cu by Ag atoms, which weakens the overall mechanical integrity of the Cu lattice.

3.2.2 Comparison at Different Temperatures

The peak stress is highest at 200K for all Ag compositions, indicating enhanced mechanical strength at lower temperatures. For 5%Ag, the peak stress attains its highest value of 8.17 GPa across all temperatures and compositions. However, as the Ag content rises to 40%, the peak stress decreases significantly, dropping to around 6.11 GPa. The stress-strain curves reveal a more distinct elastic region before the peak, indicating that dislocation motion is suppressed at lower temperatures, thereby enhancing mechanical strength. At 300K, the peak stress values decrease compared to 200K but remain higher than those at 400K. For 5%Ag, the peak stress is slightly reduced to approximately 8.0 GPa, while for 40%Ag, it drops to 6.59 GPa. The elastic region shortens slightly compared to 200K, which is attributed to increased thermal energy at 300K, allowing easier dislocation movement and reducing the overall strength. At 400K, the peak stress decreases further across all compositions. For 5%Ag, it drops to around 7.54 GPa, while for 40%Ag, it declines to 6.11 GPa. The elastic region becomes shorter, and the stress-strain curve exhibits a more gradual decline after the peak, suggesting increased plastic deformation driven by thermal activation and a reduction in lattice resistance to dislocation motion. Additionally, the linear elastic response was observed up to a maximum strain of approximately 0.035. Fig.3 clearly demonstrates that lower temperatures (200K) suppress dislocation motion, resulting in higher strength, whereas at higher temperatures (400K), the thermal energy facilitates thermal agitation, leading to a decrease in mechanical strength. The strain at failure increases slightly with increasing Ag content, suggesting that higher Ag compositions promote more plastic deformation.

3.3 Ultimate tensile strength (UTS)

Fig.4 illustrates the ultimate tensile strength (UTS) of Cu-Ag nanowires as a function of silver (Ag) composition at

three different temperatures. The ultimate tensile strength (UTS) decreases with increasing Ag composition, demonstrating a consistent trend across all temperature conditions. At lower Ag content (Cu-Ag₀₅), the UTS is highest, with values of 8.17 GPa at 200K, 7.99 GPa at 300K, and 7.54 GPa at 400K. As the Ag content increases to 20–40%, the UTS steadily declines, reaching a minimum of about 6.11 GPa at 400K for Cu-Ag₄₀. This reduction is attributed to the weakening of the Cu lattice structure caused by the addition of Ag atoms, which diminishes the material's overall mechanical strength. Furthermore, at elevated temperatures, the thermal energy increases atomic vibrations, which reduces the stability of the crystal lattice and promotes dislocation activity. This phenomenon, known as thermal softening, decreases the resistance to deformation, leading to lower UTS values. The decrease in UTS with temperature is more pronounced at higher Ag compositions, as the weakened lattice becomes more susceptible to thermal effects. Additionally, there are minimal changes in UTS for 25% and 40% Ag, indicating that beyond 20% Ag content, further increases have little impact on UTS values. These findings underscore the combined influence of temperature and Ag composition on the mechanical behavior of Cu-Ag nanowires, highlighting a trade-off between alloy composition and mechanical stability.

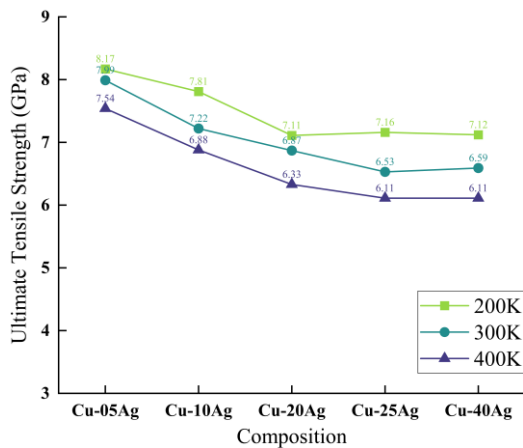


Fig.4 UTS of Cu-Ag nanowires at different temperatures and compositions.

3.4 Modulus of elasticity

Fig.5 highlights a steady increase with higher silver composition till 20% Ag composition, indicating that the addition of Ag enhances the nanowire's stiffness. The mismatch in atomic radii between Cu (1.28 Å) and Ag (1.44 Å) introduces lattice strain in the nanowire, making the atomic structure more resistant to deformation under applied stress. Silver, with its face-centered cubic (FCC) crystal structure similar to Cu, integrates well into the Cu lattice. This alloying effect strengthens the overall lattice, thereby increasing the modulus. Ag composition may lead to more homogeneous structural properties, reducing localized defects or dislocations that typically weaken the material. However, beyond 20% Ag, the rate of increase slows down, and the modulus stabilizes or slightly decreases, particularly at 400K. This behavior suggests that excessive Ag content introduces structural distortions or lattice mismatches within the Cu matrix, which can reduce the overall stiffness of the material.

At 200 K, the nanowires exhibit their highest stiffness due to minimal atomic vibrations and stronger interatomic

forces. At 400 K, the modulus decreases due to the thermal agitation, where elevated temperatures cause greater atomic vibrations as observed in most metallic systems, weakening the material's ability to resist deformation. For instance, at 20% Ag, the modulus decreases from 100.55 GPa at 200 K to 92.69 GPa at 400 K.

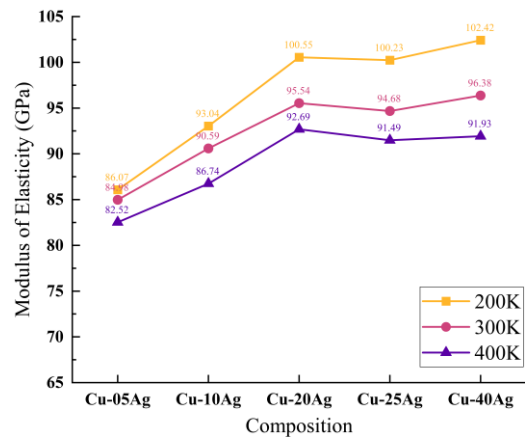


Fig.5 Modulus of elasticity of Cu-Ag nanowires at different temperatures and compositions

Interestingly, the rate of modulus decline with temperature is smaller at lower Ag compositions. For example, at 05% Ag, the modulus decreases by only 3.5 GPa between 200 K and 400 K, compared to a drop of around 10.5 GPa for 40% Ag. This suggests that as the Ag composition increases, the lattice undergoes greater structural disruptions and atomic mismatches due to the substitution of Cu atoms with Ag atoms, which have a larger atomic radius. This leads to a weaker and less stable lattice structure, making it more vulnerable to thermal vibrations at higher temperatures. As a result, the modulus of elasticity decreases more quickly with increasing temperature at higher Ag compositions. The addition of more Ag reduces the overall bonding strength in the material, intensifying the thermal softening effect.

While the peak modulus is observed at 40% Ag, the marginal difference within the 20–40% Ag range suggests 20% Ag as the optimal composition for maximizing elastic response. Beyond this composition, the stabilizing trend suggests a diminishing strengthening effect of Ag, likely due to microstructural irregularities introduced by higher solute content. Overall, the results demonstrate that both temperature and Ag composition have a significant impact on the mechanical behavior of Cu-Ag nanowires, with the 20% Ag composition at lower temperatures (200K and 300K) providing the most favorable balance of stiffness and stability.

3.5 Validation

Table 4 Comparison of nanowires properties with previous studies.

	Properties	
	UTS	Modulus of Elasticity
Previous computational study (GPa)	3 - 7.5 [9]	64.8 [21]
From this study (GPa)	6.11 - 8.17	82.52 – 102.42

Table 4 shows that, the tensile properties obtained from this study closely aligns with previous studies on Cu-Ag specimen, validating the simulation results. As there are no experimental data for Cu-Ag nanowire, data obtained from this study can be used as frame of reference for future experiment.

4. Conclusion

This study presents a comprehensive molecular dynamics study on the tensile properties of Cu-Ag nanowires, exploring the effects of silver (Ag) composition and temperature variations. The study revealed that both ultimate tensile strength (UTS) and modulus of elasticity are significantly influenced by these factors. The UTS decreased with increasing Ag content, with Cu-Ag₀₅ exhibiting the highest strength while Cu-Ag₄₀ showing the lowest. Conversely, modulus of elasticity displayed an upward trend with Ag content. Temperature negatively impacted both UTS and modulus of elasticity, with higher temperatures causing greater reductions in value. Stress-strain analysis showed linear elastic behavior up to a small strain, followed by distinct plastic deformation and necking phases. Cu-Ag₀₅ demonstrated the highest toughness, while Cu-Ag₄₀ provided superior stiffness. Beyond 20% Ag composition, both UTS and modulus of elasticity exhibit minimal variation. Therefore, Cu-Ag₂₀ could be the optimal composition for achieving the best balance of desired properties. Cu-Ag nanowires are emerging as a promising area of research, making significant strides in fields such as flexible transparent conductors, energy harvesting and storage devices, composite material reinforcement and so on.

7. Acknowledgement

The authors would like to express their gratitude to the Department of Mechanical Engineering at Chittagong University of Engineering & Technology (CUET) for their support and provision of lab facilities.

References

- [1] Royal Society (Great Britain) and Royal Academy of Engineering (Great Britain), Nanoscience and nanotechnologies: opportunities and uncertainties. Royal Society, 2004.
- [2] R. KOTTAPPARA, S. PALANTAVIDA, and B. K. VIJAYAN, "Enhanced reduction reaction by Cu-Ag core-shell nanowire catalyst," *Journal of Chemical Sciences*, vol. 132, no. 1, p. 115, Dec. 2020.
- [3] P. Yang, "30 years of semiconductor nanowire research: A Personal Journey," *Isr J Chem*, p. e202300127, 2024.
- [4] H. Y. Lee and S. Kim, "Nanowires for 2D material-based photonic and optoelectronic devices," *Nanophotonics*, vol. 11, no. 11, pp. 2571–2582, Jun. 2022.
- [5] I. E. Stewart, S. Ye, Z. Chen, P. F. Flowers, and B. J. Wiley, "Synthesis of Cu-Ag, Cu-Au, and Cu-Pt Core-Shell Nanowires and Their Use in Transparent Conducting Films," *Chemistry of Materials*, vol. 27, no. 22, pp. 7788–7794, Nov. 2015.
- [6] S. Ye *et al.*, "A rapid synthesis of high aspect ratio copper nanowires for high-performance transparent conducting films," *Chemical Communications*, vol. 50, no. 20, pp. 2562–2564, Feb. 2014.
- [7] Y. Wei, S. Chen, Y. Lin, Z. Yang, and L. Liu, "Cu-Ag core-shell nanowires for electronic skin with a petal molded microstructure," *J Mater Chem C Mater*, vol. 3, no. 37, pp. 9594–9602, Sep. 2015.
- [8] Y. Yuan, H. Xia, Y. Chen, and D. Xie, "One-step synthesis of oxidation-resistant Cu@Ag core-shell nanoparticles," *Micro Nano Lett*, vol. 13, no. 2, pp. 171–174, Feb. 2018.
- [9] P. tao Li, Y. qing Yang, X. Luo, N. Jin, G. Liu, and Y. Gao, "Structural evolution of copper-silver bimetallic nanowires with core-shell structure revealed by molecular dynamics simulations," *Comput Mater Sci*, vol. 137, pp. 289–296, Sep. 2017.
- [10] J. Sarkar and D. K. Das, "Study of the effect of varying core diameter, shell thickness and strain velocity on the tensile properties of single crystals of Cu-Ag core-shell nanowire using molecular dynamics simulations," *Journal of Nanoparticle Research*, vol. 20, no. 1, Jan. 2018.
- [11] J. Sarkar and D. K. Das, "Molecular dynamics study of defect and dislocation behaviors during tensile deformation of copper-silver core-shell nanowires with varying core diameter and shell thickness," *Journal of Nanoparticle Research*, vol. 20, no. 10, Oct. 2018.
- [12] A. P. Thompson *et al.*, "LAMMPS - a flexible simulation tool for particle-based materials modeling at the atomic, meso, and continuum scales," *Comput Phys Commun*, vol. 271, p. 108171, Feb. 2022.
- [13] A. Stukowski, "Visualization and analysis of atomistic simulation data with OVITO—the Open Visualization Tool," *Model Simul Mat Sci Eng*, vol. 18, no. 1, Jan. 2010.
- [14] T. M. Inc., "MATLAB version: 9.13.0 (R2022b)," 2022, *The MathWorks Inc., Natick, Massachusetts, United States*. [Online]. Available: <https://www.mathworks.com>
- [15] A. P. Moore, C. Deo, M. I. Baskes, M. A. Okuniewski, and D. L. McDowell, "Understanding the uncertainty of interatomic potentials' parameters and formalism," *Comput Mater Sci*, vol. 126, pp. 308–320, Jan. 2017.
- [16] K. H. Kang, I. Sa, J. C. Lee, E. Fleury, and B. J. Lee, "Atomistic modeling of the Cu-Zr-Ag bulk metallic glass system," *Scr Mater*, vol. 61, no. 8, pp. 801–804, Oct. 2009.
- [17] M.-I Baskes, "Determination of modified embedded atom method parameters for nickel," 1997.
- [18] H. Grubmüller, H. Heller, A. Windemuth, and K. Schulten, "Generalized Verlet Algorithm for Efficient Molecular Dynamics Simulations with Long-range Interactions," *Mol Simul*, vol. 6, no. 1–3, pp. 121–142, Mar. 1991.
- [19] C. Braga and K. P. Travis, "A configurational temperature Nosé-Hoover thermostat," *Journal of Chemical Physics*, vol. 123, no. 13, Oct. 2005.
- [20] D. H. Tsai, "The virial theorem and stress calculation in molecular dynamics," *J Chem Phys*, vol. 70, no. 3, pp. 1375–1382, Feb. 1979.
- [21] A. Kardani and A. Montazeri, "Temperature-based plastic deformation mechanism of Cu/Ag nanocomposites: A molecular dynamics study," *Comput Mater Sci*, vol. 144, pp. 223–231, Mar. 2018.